Thomas-Fermi Molecular-Dynamics, Linear Screening, and Mean-Field Theories of Plasmas

G. Zérah and J. Clérouin
Centre d'Etudes de Limeil-Valenton, 94195 Villeneuve St. Georges CEDEX, France

E. L. Pollock
Lawrence Livermore National Laboratory, University of California, 94550 Livermore, California 94550
(Received 8 April 1992)

Since its introduction in 1985, *ab initio* molecular dynamics has played an important role in the analysis of ionic properties of condensed-matter systems. Extending this method to a Thomas-Fermi model for plasmas, the structure and diffusion constants from molecular-dynamics simulations of the hydrogen plasma are compared to the results of approximate theories of the same model.

PACS numbers: 52.65.+z, 05.20.−y, 71.45.Jp

In 1985, while studying the vibration modes of a Thomas-Fermi model of plasma, Laughlin [1] noted the absence of numerical simulations on such systems (in contrast to the large number of simulations on liquids described by pair potentials). Such simulations would allow comparison between "rigorous" results and the numerous models commonly used in dense plasma physics, such as the one-component plasma (OCP) (see, e.g., [2]), linear screening theory [3,4], and density-functional theory coupled with an integral equation of fluids [5–7].

Car and Parrinello have presented a pseudo-Lagrangian technique to perform molecular-dynamics (MD) simulations without an effective pair potential [8]. Although this method was developed in the solid-state physics context, essentially to study *s-p* bonded materials, it can be extended to plasma physics as long as the density can be used as the only dynamical variable [9]. This restriction is necessary since we wish to consider high-temperature plasmas, where the ionization state is not prescribed but rather computed as part of the simulation, which precludes the use of wave functions. The simplest of these approximations is the Thomas-Fermi (TF) model, which can be improved by including exchange and gradient corrections.

In this Letter a tool (the TFMD model) for studying plasmas from "first principles," which is not limited by hypotheses regarding the electronic response function, the ionization state of the ions, or time averaging of the ionic motion, is described.

We present below molecular-dynamics simulations of a hydrogen plasma, for representative values of the Wigner-Seitz radius a, $(4\pi/3)a^3=\rho_i$, and of the ionic coupling parameter $\Gamma_i=e^2/ak_BT_i$ $(10\leq\Gamma_i\leq 100)$. The electronic density is characterized by r_s, the ratio of the electron sphere radius a_e to the Bohr radius, $r_s=a_e/a_B$ $(0.5\leq r_s\leq 5)$, and by a temperature T_e or equivalently by an electronic coupling parameter $\Gamma_e=e^2/a_ek_BT_e$. In these terms, the ratio of the Fermi temperature to the electronic temperature is $T_e/T_F=(\Gamma_e/2r_s)(9\pi/4)^{2/3}$. This range of parameters spans various states of the plasma, from the strongly coupled unscreened OCP ($\Gamma=100$, $r_s=0.5$) to the strongly screened collection of quasineutral atoms. In the results presented below, the effect of screening on the radial distribution function and velocity autocorrelation function is described, and compared with approximate theories for selected states of the plasma. The effect of finite electronic temperature is also investigated.

In this paper, the unit of length is the electron sphere radius a_e and energies are given in units of e^2/a_e.

Formulation of the equations of motion.—The model has already been presented in the one-dimensional case [9], while the three-dimensional version together with many numerical details is the subject of a separate publication [10]. It suffices to state here that the fictitious Lagrangian treats the electronic density and the ionic coordinates as dynamical variables, and takes the form

$$\mathcal{L}=\tfrac{1}{2}u\int\dot{\rho}^2(\mathbf{r})d\mathbf{r}+\tfrac{1}{2}M_i\sum_{i=1}^{N}\dot{\mathbf{R}}_i^2-F_0[\rho(\mathbf{r}),\mathbf{R}_i]+\Lambda\left[\int\rho(\mathbf{r})d\mathbf{r}-N\right], \tag{1}$$

where $F_0[\rho(\mathbf{r}),\mathbf{R}_i]=K[\rho(\mathbf{r})]+V[\rho(\mathbf{r}),\mathbf{R}_i]$ is the Thomas-Fermi free-energy functional, and Λ is a Lagrange multiplier which ensures neutrality. The potential term $V[\rho(\mathbf{r}),\mathbf{R}_i]$ is the classical Coulomb interaction energy of the distribution of ions and electrons. The kinetic term is given at $T_e=0$ by

$$K[\rho(\mathbf{r})]=c_k\int\rho(\mathbf{r})^{5/3}d\mathbf{r} \tag{2}$$

with

$$c_k=\tfrac{3}{10}(3\pi^2)^{2/3}/r_s\,,$$

and at finite temperature by [11,12]

$$K[\rho(\mathbf{r})]=(1/\Gamma_e)\int[\rho(\mathbf{r})\xi(\mathbf{r})-\tfrac{2}{3}\rho_0F_{3/2}(\xi)]d\mathbf{r}\,,$$
$$\xi(\mathbf{r})=F_{1/2}^{-1}(\rho(\mathbf{r})/\rho_0)\,, \tag{3}$$

where $F_i(x)$ are the usual Dirac integrals and $\rho_0=(1/2\pi^2)(2r_s/\Gamma_e)^{3/2}$.

The fictitious mass μ has to be chosen sufficiently small to ensure an adiabatic motion of the electronic density in

the varying field of the ions, in a reasonable amount of computer time. The kinetic-energy transfer between the electronic and ionic degrees of freedom is then very small, and the electron gas acts as a quasiholonomic constraint on the ions to keep them on the Born-Oppenheimer surface. As a rule of thumb, the ratio M/μ is chosen such that the ratio of characteristic frequencies of the electronic and ionic system (which controls energy transfer) is about 20. A good description of electronic pseudodynamics and the mass ratio imposes a time step of $10^{-3}\omega_p^{-1}$, where ω_p is the ion plasma frequency.

The density is represented on a grid of 32^3 points, and the simulation is done in real space, except for the Poisson equation, which is solved by Fourier transform. To avoid huge forces when an ion passes near a grid point, the Coulomb-Ewald potential is regularized at the origin, by smearing the ionic core; that is, it is replaced by a parabola near the ionic nucleus, for $r \leq r_c$. We have checked that, provided r_c is chosen sufficiently small $(0.1r_s)$, this does not affect significantly ionic dynamics [10].

For a system of 54 ions, the total-energy conservation during a run of 20000 time steps is better than 10^{-5} and no significant drift is observed in the pseudo kinetic energy which remains 3 orders of magnitude smaller than the ionic kinetic energy. At $\Gamma=50$ and $r_s=1$ a mass ratio $M/\mu=250$ was used. This was increased to $M/\mu=1000$ for higher temperature plasmas of $\Gamma=10$ and $r_s=1$. The fact that no negative densities were encountered is an additional test of adiabaticity.

Simulation of hydrogen.—Since there exists many published results on approximate theories [7] (including the Thomas-Fermi theory) of the hydrogen plasma, we present results for this element, although it is not the most appropriate for an application of Thomas-Fermi theory. One of the most complete plasma models to compare our results with is the hypernetted-chain theory, where the average electronic and ionic density around an ion are computed under the assumptions (i) that the electronic density can be computed in the field produced by the central ion and the average distribution of neighboring ions, and (ii) that the average distribution of ions around a central ion can be computed via, for instance, the hypernetted-chain (HNC) integral equation, using the pair potential obtained by integrating out the electronic degrees of freedom.

When the first step is performed using TF theory, and the second using HNC theory, the corresponding model is referred to as the TFHNC model. We can also define the TFPY model for the Percus-Yevick equation.

Ionic distribution function.—At high density, where the Fermi kinetic energy is much higher than the Coulomb potential energy (e.g., $r_s=0.5$), the pair distribution function $g(r)$ computed with the TFMD model is indistinguishable from the OCP $g(r)$ of Sahlin, Brush, and Teller [13]. TFHNC also yields the same pair correlation function, a result that can be related to the fact that mean-field theories are exact at high densities, where linear response applies [7].

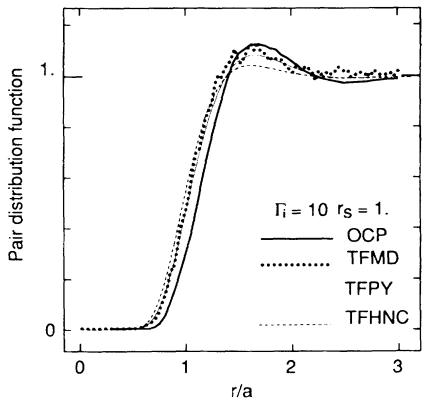

FIG. 1. Pair correlation function $g(r)$ computed at $\Gamma_i=10$ and $r_s=1$, for the OCP model (bold line), TFMD model (dots), TFPY (thin line), and TFHNC (dashed line).

At lower density, screening effects cause significant differences as shown in Fig. 1 where $g(r)$ for $r_s=1$ and $\Gamma=10$ is plotted. The first maximum and the first contact point of $g(r)$, given by the TFMD calculation, are now shifted to smaller values, compared to the OCP result. These features are well reproduced by the TFPY calculation while the TFHNC calculation underestimates the value of the first peak.

In Fig. 2, we present results at $r_s=5$, $\Gamma=50$ where screening is still more dramatic. In this case, the OCP calculation is clearly inaccurate, and we encountered convergence problems with the TFHNC theory. No phase transition associated with these convergence problems in the TFHNC model, as was suggested by various authors [8], was observed. A calculation using a screened potential with the Thomas-Fermi screening length $\lambda_{TF}/a_i = (\pi/12Z)^{1/3} r_s^{-1/2}$ (referred to as LSMD) underesti-

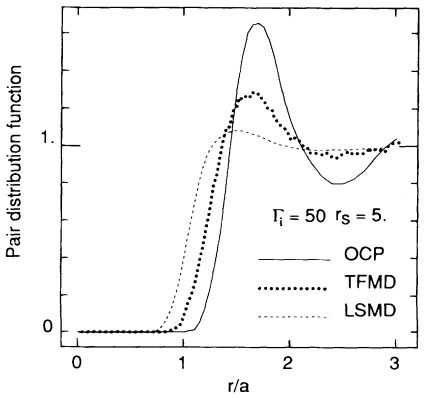

FIG. 2. Pair correlation function $g(r)$ computed at $\Gamma_i=50$ and $r_s=5$ for the OCP model (solid line), TFMD (dots), and LSMD model (dashed line).

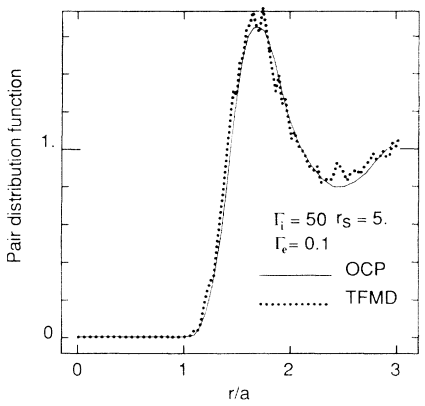

FIG. 3. Comparison between the pair correlation function computed for the OCP model at $\Gamma_i = 50$ (solid line), with TFMD at $r_s = 5$ and electronic temperature characterized by an electronic coupling $\Gamma_e = 0.1$ (dots).

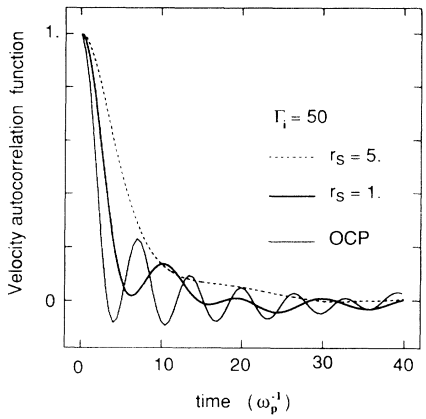

FIG. 4. Velocity autocorrelation function $Z(t)$ computed at $\Gamma_i = 50$, for the OCP model (thin line), TFMD model at $r_s = 1$ (bold line), and TFMD model at $r_s = 5$ (dashed line).

mates strongly the height of the first peak of $g(r)$, but better results can be achieved if we use an empirical renormalized screening length $\lambda_{TF}^{*} = 1.6\lambda_{TF}$. The same empirical renormalization has been also proposed by other authors [14] to reproduce accurately the pair correlation functions of expanded liquid metals.

Since at strong coupling, $T \ll T_F$, all the preceding simulations were performed at zero electronic temperature. To demonstrate finite-electronic-temperature effects, the electronic temperature was raised to $T_e = 5T_F$ while keeping the ionic temperature constant. Such a nonequilibrium situation can be encountered during ultrashort laser-matter interactions [15]. We observe now a temperature driven ionization, and indeed, apart from statistical noise, it is clear in Fig. 3 that at $r_s = 5$, $\Gamma_i = 50$, and $\Gamma_e = 0.1$, the TFMD model again yields the OCP pair distribution function. This was expected, since the electron gas is again highly kinetic and therefore nearly uniform.

Velocity autocorrelation function and diffusion coefficient.—The effective pair potential computed in a mean-field approach such as TFHNC is not expected to yield as accurate results for dynamics as for the static case, since it assumes a spherically averaged neighborhood for the central ion. In particular, the damping of the oscillations in the velocity autocorrelation function due to screening is the central quantity of interest.

We have computed the velocity autocorrelation function $Z(t)$ from our simulations and made comparison with mean-field and OCP models. At strong coupling ($\Gamma_i = 50$), $Z(t)$ computed for the OCP model exhibits oscillations close to the plasma frequency which is due to a coupling between individual motion and collective modes [16]. As the density is lowered ($r_s = 1$), the screened ionic interaction can be interpreted in term of an effective charge Z^* smaller than the unscreened one, and hence coupled with a lower collective frequency (Fig. 4). For $r_s = 5$, there is almost no trace of collective effects.

A quantitative measure of the effect of screening is given in Table I, by the variation of the diffusion coefficient $D = \int_0^\infty Z(t)dt$, which is 3 times larger for $r_s = 5$ than the OCP value (corresponding to $r_s = 0$).

The linear screened Thomas-Fermi potential yields too large a diffusion constant. But the empirical screening length λ_{TF}^{*}, which reproduces the pair correlation function, also yields a rather good diffusion constant (Table I).

Simulations at low coupling ($\Gamma_i = 10$, $r_s = 1$) were also performed to study the ability of the mean-field potential to reproduce dynamical properties in this regime. In Fig. 5, $Z(t)$ computed from a TFMD simulation is compared with molecular-dynamics simulations using the pair potential generated by TFHNC calculations (denoted as MFPOT). While the TFMD velocity autocorrelation function still exhibits damped oscillations [compare the first maximum of $Z(t)$ for $r_s = 1$ in Figs. 4 and 5] the MFPOT calculation produces a totally damped velocity autocorrelation function, a fact which is attributable to

TABLE I. Diffusion constant in reduced units $D^* = D/a^2\omega_p$ vs r_s and coupling Γ. MD λ_{TF}^{*} stands for molecular dynamics with the empirical Thomas-Fermi screening length and MFPOT to molecular dynamics using the potential generated by HNC calculations.

	OCP $r_s = 0$	$r_s = 1$	$r_s = 5$
$\Gamma = 50$			
TFMD	0.015	0.021	0.046
MD λ_{TF}^{*}			0.042
$\Gamma = 10$			
TFMD	0.134	0.164	
MFPOT		0.166	

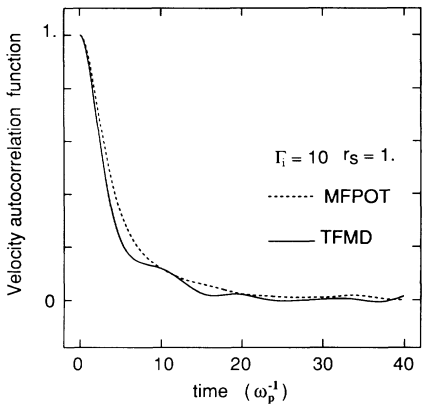

FIG. 5. Velocity autocorrelation function $Z(t)$ computed at $\Gamma_i = 10$ and at $r_s = 1$ with TFMD model (solid line) and MFPOT model (dashed line).

overscreening of the ionic charge. Nevertheless, the diffusion coefficients are very close in both cases.

In this Letter, a method for simulating the static and *dynamical* properties of dense plasmas, which includes self-consistently the response of the electronic density to the ionic motion, was presented. These simulations provide much more information than previous models where the ions are kept *fixed* [17]. Comparing the results with some approximations commonly used in plasma physics, sizable effects on the radial distribution function and diffusion coefficient are observed. The inclusion of gradient and exchange corrections is straightforward, and should allow one to compute accurate values for the equation of state, transport properties, and local environment in mixtures. The results of these calculations, which are under way, will be the subject of a future publication.

Discussions with J. P. Hansen, P. Dallot, E. Paci, and G. Cicotti are gratefully acknowledged.

[1] R. B. Laughlin, Phys. Rev. A **33**, 510 (1986).
[2] M. Baus and J. P. Hansen, Phys. Rep. **59**, 1 (1980).
[3] G. M. Torrie, J. P. Hansen, and P. Vieillefosse, Phys. Rev. A **16**, 2153 (1977).
[4] H. Iyetomi and S. Ichimaru, Phys. Rev. A **34**, 433 (1986).
[5] J. Chihara, Prog. Theor. Phys. **60**, 1640 (1978).
[6] M. W. C. Dharma-Wardana and F. Perrot, Phys. Rev. A **26**, 2096 (1982).
[7] D. Ofer, E. Nardi, and Y. Rosenfeld, Phys. Rev. A **38**, 5801 (1988).
[8] R. Car and M. Parrinello, Phys. Rev. Lett. **55**, 3471 (1985).
[9] J. Clérouin, G. Zérah, D. Bénisti, and J. P. Hansen, Europhys. Lett. **13**, 685 (1990).
[10] J. Clérouin, E. L. Pollock, and P. G. Zérah, Phys. Rev. A (to be published).
[11] R. M. More, Phys. Rev. A **19**, 1234 (1979).
[12] N. M. March, Adv. Phys. **6**, 1 (1957).
[13] H. L. Sahlin, S. G. Brush, and E. Teller, J. Chem. Phys. **45**, 2102 (1966).
[14] J. P. Hansen and F. Yoshida, J. Phys. Condens. Matter **3**, 2583 (1991).
[15] M. D. Perry, *Energy and Technology Review* (Lawrence Livermore Laboratory, Berkeley, CA, 1988), p. 9.
[16] J. P. Hansen, I. R. McDonald, and E. L. Pollock, Phys. Rev. A **11**, 1025 (1975).
[17] S. Nagano, Phys. Lett. A **156**, 493 (1991).